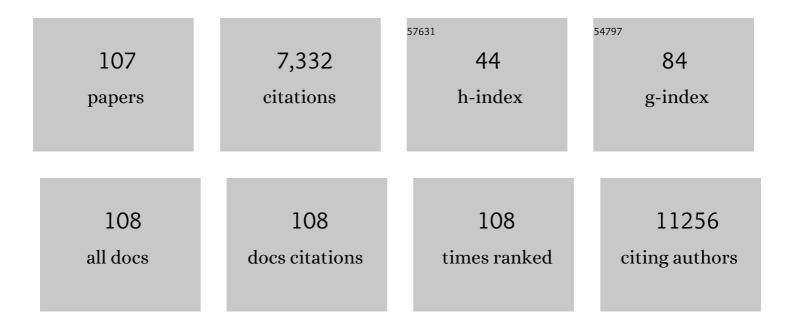
Zhenpeng Hu

List of Publications by Year in descending order

Source: https://exaly.com/author-pdf/6448208/publications.pdf Version: 2024-02-01



ZHENDENC HIL

#	Article	IF	CITATIONS
1	Homogeneous-like Alkyne Selective Hydrogenation Catalyzed by Cationic Nickel Confined in Zeolite. CCS Chemistry, 2022, 4, 949-962.	4.6	20
2	Atomic‣cale Characterization of Negative Differential Resistance in Ferroelectric Bi ₂ WO ₆ . Advanced Functional Materials, 2022, 32, 2105256.	7.8	6
3	Anisotropic black phosphorene nanotube anodes afford ultrafast kinetic rate or extra capacities for Li-ion batteries. Chinese Chemical Letters, 2022, 33, 3842-3848.	4.8	4
4	Two-Dimensional Layered Green Phosphorus as an Anode Material for Li-Ion Batteries. ACS Applied Energy Materials, 2022, 5, 2184-2191.	2.5	6
5	A first-principles study on the electrochemical reaction activity of 3d transition metal single-atom catalysts in nitrogen-doped graphene: Trends and hints. EScience, 2022, 2, 219-226.	25.0	51
6	Pt Atom on the Wall of Atomic Layer Deposition (ALD)â€Made MoS ₂ Nanotubes for Efficient Hydrogen Evolution. Small, 2022, 18, e2105129.	5.2	29
7	Ultrathin Van der Waals Antiferromagnet CrTe ₃ for Fabrication of Inâ€Plane CrTe ₃ /CrTe ₂ Monolayer Magnetic Heterostructures. Advanced Materials, 2022, 34, e2200236.	11.1	17
8	Complex spin Hamiltonian represented by an artificial neural network. Physical Review B, 2022, 105, .	1.1	8
9	V "Bridged―CoO to Eliminate Charge Transfer Barriers and Drive Lattice Oxygen Oxidation during Waterâ€Splitting. Advanced Functional Materials, 2021, 31, 2008822.	7.8	40
10	Designing a Family of Aluminum-Containing Fluoroborate Crystals with Enhanced Birefringence and Second-Harmonic Generation Coefficients Based on the First-Principles Methods. Journal of Physical Chemistry C, 2021, 125, 7431-7438.	1.5	3
11	Atomic Cobalt Vacancyâ€Cluster Enabling Optimized Electronic Structure for Efficient Water Splitting. Advanced Functional Materials, 2021, 31, 2101797.	7.8	26
12	Pd–Pt Tesseracts for the Oxygen Reduction Reaction. Journal of the American Chemical Society, 2021, 143, 496-503.	6.6	100
13	Activating Inert Surface Pt Single Atoms via Subsurface Doping for Oxygen Reduction Reaction. Nano Letters, 2021, 21, 7970-7978.	4.5	33
14	HSH-C10: A new quasi-2D carbon allotrope with a honeycomb-star-honeycomb lattice. Chinese Chemical Letters, 2021, , .	4.8	3
15	Auxetic two-dimensional transition metal selenides and halides. Npj Computational Materials, 2020, 6, .	3.5	27
16	Computational Study of a Novel 2D Ferromagnetic Metal: the Ce 2 C Monolayer. Physica Status Solidi - Rapid Research Letters, 2020, 14, 2000324.	1.2	2
17	Regular Arrangement of Two-Dimensional Clusters of Blue Phosphorene on Ag(111). Chinese Physics Letters, 2020, 37, 096803.	1.3	17
18	Reaction Pathways for α-Ga2O3 and β-Ga2O3 Phase Transition under Pressure up to 40 GPa: A First-Principles Study. Journal of Physical Chemistry C, 2020, 124, 23280-23286.	1.5	6

#	Article	IF	CITATIONS
19	Wellâ€Defined Singleâ€Atom Cobalt Catalyst for Electrocatalytic Flue Gas CO ₂ Reduction. Small, 2020, 16, e2001896.	5.2	85
20	Experimental Realization of Two-Dimensional Buckled Lieb Lattice. Nano Letters, 2020, 20, 2537-2543.	4.5	12
21	Reversible Potassium Intercalation in Blue Phosphorene–Au Network Driven by an Electric Field. Journal of Physical Chemistry Letters, 2020, 11, 5584-5590.	2.1	5
22	Pauling's rules guided Monte Carlo search (PAMCARS): A shortcut of predicting inorganic crystal structures. Computer Physics Communications, 2020, 256, 107486.	3.0	4
23	Surface Nitrogen-Injection Engineering for High Formation Rate of CO ₂ Reduction to Formate. Nano Letters, 2020, 20, 6097-6103.	4.5	71
24	Corrugation Matters: Structure Models of Single Layer Heptazine-Based Graphitic Carbon Nitride from First-Principles Studies. Journal of Physical Chemistry C, 2020, 124, 4644-4651.	1.5	19
25	The Crucial Role of Charge Accumulation and Spin Polarization in Activating Carbonâ€Based Catalysts for Electrocatalytic Nitrogen Reduction. Angewandte Chemie, 2020, 132, 4555-4561.	1.6	8
26	The Crucial Role of Charge Accumulation and Spin Polarization in Activating Carbonâ€Based Catalysts for Electrocatalytic Nitrogen Reduction. Angewandte Chemie - International Edition, 2020, 59, 4525-4531.	7.2	149
27	Rational Design of Spinel Cobalt Vanadate Oxide Co ₂ VO ₄ for Superior Electrocatalysis. Advanced Materials, 2020, 32, e1907168.	11.1	134
28	Correlation-driven eightfold magnetic anisotropy in a two-dimensional oxide monolayer. Science Advances, 2020, 6, eaay0114.	4.7	43
29	Electronic and geometric factors affecting oxygen vacancy formation on CeO2(111) surfaces: A first-principles study from trivalent metal doping cases. Applied Surface Science, 2019, 497, 143732.	3.1	14
30	Quadruple perovskite ruthenate as a highly efficient catalyst for acidic water oxidation. Nature Communications, 2019, 10, 3809.	5.8	150
31	Synthesis, structure and characterization of M(IO ₃) ₂ (HIO ₃) (M =) Tj ETQ Transactions, 2019, 48, 13074-13080.	q1 1 0.784 1.6	4314 rgBT /〇 7
32	Growth and theoretical study on the deep-ultraviolet transparent β-CsBa ₂ (PO ₃) ₅ nonlinear optical crystal. CrystEngComm, 2019, 21, 4690-4695. So the bright and dark exciten indecesse and time structure of complements.	1.3	8
33	xmlns:mml="http://www.w3.org/1998/Math/MathML"> <mml:msub><mml:mi>MoS</mml:mi><mml:mn>2using <mml:math xmlns:mml="http://www.w3.org/1998/Math/MathML"><mml:mrow><mml:msub><mml:mi mathyariant="normal">G<mml:mn>0</mml:mn></mml:mi </mml:msub><mml:msub><mml:mi< td=""><td>mn> 1.1</td><td>nl:msub>15</td></mml:mi<></mml:msub></mml:mrow></mml:math </mml:mn></mml:msub>	mn> 1.1	nl:msub>15
34	General I€â€Electronâ€Assisted Strategy for Ir, Pt, Ru, Pd, Fe, Ni Singleâ€Atom Electrocatalysts with Bifunctional Active Sites for Highly Efficient Water Splitting. Angewandte Chemie - International Edition, 2019, 58, 11868-11873.	7.2	229
35	General Ï€â€Electronâ€Assisted Strategy for Ir, Pt, Ru, Pd, Fe, Ni Singleâ€Atom Electrocatalysts with Bifunctional Active Sites for Highly Efficient Water Splitting. Angewandte Chemie, 2019, 131, 11994-11999.	1.6	28
36	Single Mo ₁ (Cr ₁) Atom on Nitrogen-Doped Graphene Enables Highly Selective Electroreduction of Nitrogen into Ammonia. ACS Catalysis, 2019, 9, 3419-3425.	5.5	258

#	Article	IF	CITATIONS
37	Chemical state of surrounding iron species affects the activity of Fe-Nx for electrocatalytic oxygen reduction. Applied Catalysis B: Environmental, 2019, 251, 240-246.	10.8	101
38	gt-C3N4 coordinated single atom as an efficient electrocatalyst for nitrogen reduction reaction. Nano Research, 2019, 12, 1181-1186.	5.8	87
39	A Dualâ€Stimuliâ€Responsive Coordination Network Featuring Reversible Wideâ€Range Luminescenceâ€Tuning Behavior. Angewandte Chemie, 2019, 131, 5670-5674.	1.6	24
40	The Quasiâ€Ptâ€Allotrope Catalyst: Hollow PtCo@singleâ€Atom Pt ₁ on Nitrogenâ€Doped Carbon toward Superior Oxygen Reduction. Advanced Functional Materials, 2019, 29, 1807340.	7.8	97
41	A Dualâ€Stimuliâ€Responsive Coordination Network Featuring Reversible Wideâ€Range Luminescenceâ€Tuning Behavior. Angewandte Chemie - International Edition, 2019, 58, 5614-5618.	7.2	132
42	Efficient energy gap tuning for T-carbon via single atomic doping. Chemical Physics, 2019, 518, 69-73.	0.9	13
43	Activating Titania for Efficient Electrocatalysis by Vacancy Engineering. ACS Catalysis, 2018, 8, 4288-4293.	5.5	141
44	Realization of flat band with possible nontrivial topology in electronic Kagome lattice. Science Advances, 2018, 4, eaau4511.	4.7	131
45	Magnetic origin of phase stability in cubic Î ³ -MoN. Applied Physics Letters, 2018, 113, 221901.	1.5	6
46	Atomic-level structure engineering of metal oxides for high-rate oxygen intercalation pseudocapacitance. Science Advances, 2018, 4, eaau6261.	4.7	164
47	An amorphous tin-based nanohybrid for ultra-stable sodium storage. Journal of Materials Chemistry A, 2018, 6, 18920-18927.	5.2	22
48	Dirac Signature in Germanene on Semiconducting Substrate. Advanced Science, 2018, 5, 1800207.	5.6	59
49	Band Gap Modulated by Electronic Superlattice in Blue Phosphorene. ACS Nano, 2018, 12, 5059-5065.	7.3	92
50	The origin of the enhanced photocatalytic activity of carbon nitride nanotubes: a first-principles study. Journal of Materials Chemistry A, 2017, 5, 4827-4834.	5.2	50
51	Imaging metal-like monoclinic phase stabilized by surface coordination effect in vanadium dioxide nanobeam. Nature Communications, 2017, 8, 15561.	5.8	33
52	Screw dislocation-driven t-Ba ₂ V ₂ O ₇ helical meso/nanosquares: microwave irradiation assisted-SDBS fabrication and their unique magnetic properties. Journal of Materials Chemistry C, 2017, 5, 6336-6342.	2.7	13
53	Frontispiz: Supported Rhodium Catalysts for Ammonia–Borane Hydrolysis: Dependence of the Catalytic Activity on the Highest Occupied State of the Single Rhodium Atoms. Angewandte Chemie, 2017, 129, .	1.6	0
54	Frontispiece: Supported Rhodium Catalysts for Ammonia–Borane Hydrolysis: Dependence of the Catalytic Activity on the Highest Occupied State of the Single Rhodium Atoms. Angewandte Chemie - International Edition, 2017, 56, .	7.2	0

#	Article	IF	CITATIONS
55	Supported Rhodium Catalysts for Ammonia–Borane Hydrolysis: Dependence of the Catalytic Activity on the Highest Occupied State of the Single Rhodium Atoms. Angewandte Chemie, 2017, 129, 4790-4796.	1.6	27
56	Supported Rhodium Catalysts for Ammonia–Borane Hydrolysis: Dependence of the Catalytic Activity on the Highest Occupied State of the Single Rhodium Atoms. Angewandte Chemie - International Edition, 2017, 56, 4712-4718.	7.2	173
57	Atomically and Electronically Coupled Pt and CoO Hybrid Nanocatalysts for Enhanced Electrocatalytic Performance. Advanced Materials, 2017, 29, 1604607.	11.1	224
58	Synergistic Effects between Doped Nitrogen and Phosphorus in Metal-Free Cathode for Zinc-Air Battery from Covalent Organic Frameworks Coated CNT. ACS Applied Materials & Interfaces, 2017, 9, 44519-44528.	4.0	65
59	Activating cobalt(II) oxide nanorods for efficient electrocatalysis by strain engineering. Nature Communications, 2017, 8, 1509.	5.8	361
60	DFT+ <i>U</i> Analysis on Stability of Low-Index Facets in Hexagonal LaCoO3 Perovskite: Effect of Co3+ Spin States. Chinese Journal of Chemical Physics, 2017, 30, 295-302.	0.6	9
61	Water Splitting: Strongly Coupled Nafion Molecules and Ordered Porous CdS Networks for Enhanced Visible-Light Photoelectrochemical Hydrogen Evolution (Adv. Mater. 24/2016). Advanced Materials, 2016, 28, 4943-4943.	11.1	0
62	Hydrogen Treatment for Superparamagnetic VO ₂ Nanowires with Large Roomâ€Temperature Magnetoresistance. Angewandte Chemie, 2016, 128, 8150-8154.	1.6	6
63	Hydrogen Treatment for Superparamagnetic VO ₂ Nanowires with Large Roomâ€Temperature Magnetoresistance. Angewandte Chemie - International Edition, 2016, 55, 8018-8022.	7.2	37
64	Strongly Coupled Nafion Molecules and Ordered Porous CdS Networks for Enhanced Visibleâ€Light Photoelectrochemical Hydrogen Evolution. Advanced Materials, 2016, 28, 4935-4942.	11.1	95
65	A first-principles study on Al-doped ZnO growth polarity on sapphire (0001) surface. Europhysics Letters, 2016, 114, 66003.	0.7	1
66	Engineering electrocatalytic activity in nanosized perovskite cobaltite through surface spin-state transition. Nature Communications, 2016, 7, 11510.	5.8	316
67	Engineering surface atomic structure of single-crystal cobalt (II) oxide nanorods for superior electrocatalysis. Nature Communications, 2016, 7, 12876.	5.8	568
68	Construction of a polyhedron decorated MOF with a unique network through the combination of two classic secondary building units. Chemical Communications, 2016, 52, 2079-2082.	2.2	36
69	Synergistic Effect of Titanate-Anatase Heterostructure and Hydrogenation-Induced Surface Disorder on Photocatalytic Water Splitting. ACS Catalysis, 2015, 5, 1708-1716.	5.5	92
70	In situ unravelling structural modulation across the charge-density-wave transition in vanadium disulfide. Physical Chemistry Chemical Physics, 2015, 17, 13333-13339.	1.3	24
71	A promising way to open an energy gap in bilayer graphene. Nanoscale, 2015, 7, 17096-17101.	2.8	13
72	Metallic mesocrystal nanosheets of vanadium nitride for high-performance all-solid-state pseudocapacitors. Nano Research, 2015, 8, 193-200.	5.8	50

#	Article	IF	CITATIONS
73	Ultrahigh Infrared Photoresponse from Core–Shell Singleâ€Domainâ€VO ₂ /V ₂ O ₅ Heterostructure in Nanobeam. Advanced Functional Materials, 2014, 24, 1821-1830.	7.8	87
74	The Key Role of van der Waals Interactions in MPc/Au(111) (M = Co, Fe, H ₂) Systems Based on First-Principles Calculations. Journal of Physical Chemistry C, 2014, 118, 27843-27849.	1.5	14
75	Ir Detectors: Ultrahigh Infrared Photoresponse from Core-Shell Single-Domain-VO2/V2O5Heterostructure in Nanobeam (Adv. Funct. Mater. 13/2014). Advanced Functional Materials, 2014, 24, 1820-1820.	7.8	2
76	Efficient Method for Fast Simulation of Scanning Tunneling Microscopy with a Tip Effect. Journal of Physical Chemistry A, 2014, 118, 8953-8959.	1.1	7
77	Substrate engineering in stabilizing epitaxial MgO(1 1 1) polar ultrathin films: first-principles calculations. Journal of Physics Condensed Matter, 2014, 26, 315014.	0.7	0
78	Tunable Band Structures of Heterostructured Bilayers with Transition-Metal Dichalcogenide and MXene Monolayer. Journal of Physical Chemistry C, 2014, 118, 5593-5599.	1.5	147
79	Dimerization of boron dopant in diamond (100) epitaxy induced by strong pair correlation on the surface. Journal of Physics Condensed Matter, 2013, 25, 045011.	0.7	3
80	The atomic structures of carbon nitride sheets for cathode oxygen reduction catalysis. Journal of Chemical Physics, 2013, 138, 164706.	1.2	19
81	Passivating a transition-metal surface for more uniform growth of graphene: Effect of Au alloying on Ni(111). Physical Review B, 2013, 87, .	1.1	7
82	Coverage-dependent Orientations of Dy@C82Molecules on Au(111) Surface. Chinese Journal of Chemical Physics, 2012, 25, 423-428.	0.6	5
83	Writing charge into the <i>n</i> -type LaAlO3/SrTiO3 interface: A theoretical study of the H2O kinetics on the top AlO2 surface. Applied Physics Letters, 2012, 101, .	1.5	8
84	Tuning the catalytic property of nitrogen-doped graphene for cathode oxygen reduction reaction. Physical Review B, 2012, 85, .	1.1	81
85	Hexamethoxytribenzocoronene, a Janus Double Concave Molecule to Selectively Assemble with Fullerene C60. Chemistry Letters, 2012, 41, 1588-1590.	0.7	4
86	Hydrodebromination and Oligomerization of Dibromomethane. ACS Catalysis, 2012, 2, 479-486.	5.5	28
87	Two-Dimensional Superlattice: Modulation of Band Gaps in Graphene-Based Monolayer Carbon Superlattices. Journal of Physical Chemistry Letters, 2012, 3, 3373-3378.	2.1	60
88	Interactions in different domains of truxenone supramolecular assembly on Au(111). Physical Chemistry Chemical Physics, 2012, 14, 3980.	1.3	8
89	Halogen Adsorption on CeO ₂ : The Role of Lewis Acid–Base Pairing. Journal of Physical Chemistry C, 2012, 116, 6664-6671.	1.5	48
90	Chemistry of Lewis Acid–Base Pairs on Oxide Surfaces. Journal of Physical Chemistry C, 2012, 116, 10439-10450.	1.5	293

#	Article	IF	CITATIONS
91	Effect of Dopants on the Energy of Oxygen-Vacancy Formation at the Surface of Ceria: Local or Global?. Journal of Physical Chemistry C, 2011, 115, 17898-17909.	1.5	118
92	Choice of <i>U</i> for DFT+ <i>U</i> Calculations for Titanium Oxides. Journal of Physical Chemistry C, 2011, 115, 5841-5845.	1.5	264
93	Chemistry of Doped Oxides: The Activation of Surface Oxygen and the Chemical Compensation Effect. Journal of Physical Chemistry C, 2011, 115, 3065-3074.	1.5	102
94	CO2 methanation on Ru-doped ceria. Journal of Catalysis, 2011, 278, 297-309.	3.1	328
95	STM characterization of size-selected V1, V2, VO, and VO2 clusters on a TiO2(110)-(1×1) surface at room temperature. Surface Science, 2011, 605, 972-976.	0.8	27
96	Scanning Tunneling Spectroscopy of Metal Phthalocyanines on a Au(111) Surface with a Ni Tip. Chinese Physics Letters, 2011, 28, 076802.	1.3	0
97	Methane complete and partial oxidation catalyzed by Pt-doped CeO2. Journal of Catalysis, 2010, 273, 125-137.	3.1	186
98	Identification of metal-cage coupling in a single metallofullerene by inelastic electron tunneling spectroscopy. Applied Physics Letters, 2010, 96, 253110.	1.5	9
99	Electronic and Magnetic Properties of Metal Phthalocyanines on Au(111) Surface: A First-Principles Study. Journal of Physical Chemistry C, 2008, 112, 13650-13655.	1.5	81
100	Synthetic paramontroseite VO2 with good aqueous lithium–ion battery performance. Chemical Communications, 2008, , 3891.	2.2	102
101	Detecting a Moleculeâ^'Surface Hybrid State by an Fe-Coated Tip with a Non-s-Like Orbital. Journal of Physical Chemistry C, 2008, 112, 15603-15606.	1.5	14
102	Identifying atomic geometry and electronic structure of (2×3)-Sr/Si(100) surface and its initial oxidation. Journal of Chemical Physics, 2008, 129, 164707.	1.2	22
103	Kondo effect in single cobalt phthalocyanine molecules adsorbed on Au(111) monoatomic steps. Journal of Chemical Physics, 2008, 128, 234705.	1.2	44
104	Observation of Hierarchical Chiral Structures in 8-Nitrospiropyran Monolayers. Journal of Physical Chemistry B, 2007, 111, 6973-6977.	1.2	23
105	Hexagonal Cu2SnS3 with metallic character: Another category of conducting sulfides. Applied Physics Letters, 2007, 91, .	1.5	85
106	Mechanism for Negative Differential Resistance in Molecular Electronic Devices: Local Orbital Symmetry Matching. Physical Review Letters, 2007, 99, 146803.	2.9	150
107	Quasi Chiral Phase Separation in a Two-Dimensional Orientationally Disordered System:Â 6-Nitrospiropyran on Au(111). Journal of the American Chemical Society, 2007, 129, 3857-3862.	6.6	57